Atomic-scale study of dry sliding friction

A. Buldum and S. Ciraci
Department of Physics, Bilkent University, Bilkent 06533, Ankara, Turkey
(Received 17 June 1996; revised manuscript received 25 September 1996)

We present a theoretical study of dry sliding friction, which has a close bearing on the experiments done by using the atomic and friction force microscope. By performing atomic-scale calculations for the friction between a single atom and monoatomic infinite chain, we examined the effect of various material parameters on the stick-slip motion. We found that the perpendicular elastic deformation of the substrate that is induced by the sliding object is crucial for the energy damping in friction. In this case, the average friction force strongly depends on the perpendicular force constant of the substrate and the friction constant varies with the normal force. In particular, soft materials that continue to be elastic for a wide range of perpendicular compression may exhibit a second state. As a result, the hysteresis curve in the stick-slip motion becomes anisotropic. [S0163-1829(97)04804-2]

I. INTRODUCTION

The relative motion of two objects at close proximity (sliding, rolling, or motion in the perpendicular direction) induces nonconservative forces that resist the motion. This phenomenon is called friction and is relevant for various disciplines in science and technology.[1–4] The origin of the friction force, and the energy damping therefrom, is the short- and long-range interactions between two objects. Depending on the distance between objects and also on their relative lateral positions, the magnitude of the interaction potential varies and it can be either attractive or repulsive. The invention of the atomic force microscope[5] (AFM) and the frictional force microscope[6,7] (FFM) has made an important impact on the science of friction or tribology. Nowadays, perpendicular and lateral atomic forces in the range of nanonewtons (which is 10^{-9} N and 0.62415 eV/Å) can be measured with precision by using these microscopes.[8–10]

The moving objects either are in direct contact through the asperities or lubricants are introduced between them to reduce friction. In boundary lubrication, foreign atoms with monolayer coverage prevent the surfaces of moving objects from making adhesive contact. The dry sliding friction between atomically flat, commensurate or incommensurate sliding surfaces perhaps is the simplest but most fundamental type of friction in tribology. Depending on the conditions, it may include several interesting phenomena such as adhesion, wetting and atom transfer, strain-induced phase transition and local surface reconstruction, anisotropy in stick-slip motion, and dissipation of a local, nonequilibrium distribution of phonons. Whatever the type and the scale of the friction, the atomic process between the sliding or moving objects is crucial for friction.[11] During various atomic processes the energy of motion is damped by phononic and electronic mechanisms. The nonequilibrium phonon density created locally in the course of sliding is dissipated by phonon-phonon and electron-phonon coupling. The energy dissipation may involve also electron-hole creation and charge-density waves.[12]

Experimental investigations of the interaction between solid surfaces in dry friction and between surface and lubricant atoms in boundary lubrication have shed light on the underlying microscopic mechanism of friction. In the meantime, theoretical studies using atomic models[13–18] and large-scale molecular-dynamics simulations[19–21] have provided insight for a better understanding. Nowadays, researchers have come up with interesting results such as a superlubricant state at high sliding velocities[22] and the possibility of the nearly frictionless sliding in mesoscopic solids.[23]

The atomic-scale analysis of the interaction between sliding surfaces is necessary to understand the nonconservative lateral forces and the mechanism of energy dissipation in friction. It is hoped that with the knowledge gained this way one will able to provide means towards a better control of friction and hence reduce the loss of energy. With this motivation our study presents an analysis of the interaction in dry sliding friction. First, the nature of the interactions and lateral and perpendicular forces generated therefrom are discussed. The effect of the lateral and perpendicular deformations that are induced by a sliding object (represented by a single atom) on an infinite atomic chain is investigated. The present model is comprised of features that were not included in the models used in the earlier theoretical studies. The results obtained from this work indicate that the elasticity of the surface in the perpendicular direction has a significant effect on the friction and may give rise to a second state for a certain range of elastic constants and normal force.

II. NATURE OF INTERACTIONS BETWEEN SLIDING SURFACES

Short-range and long-range interactions occur between the surfaces of sliding objects. The short-range interaction is comprised of the Coulomb repulsion of ions and the attractive electron-ion interaction.[2] In spite of the fact that repulsive interaction is long ranged, it is screened by the electronic charge density that decays exponentially above the surface. The interaction energy $E_i(\vec{r})$ between two atomically flat and commensurate metal slabs (A and B) can be obtained by comparing the total energies[24] of the individual slabs with the total energy of two interacting slabs ($A+B$). The relative position of the slabs is given by the vector

$\vec{r}=\vec{r}(x,y,z)$ between two points O_A and O_B fixed in the slabs A and B, respectively. It is assumed that these points are far from the interaction region, so they are not affected by the induced deformations in A and B. For a given separation $z=z_0$, $E_i(x,y,z_0)$ has a two-dimensional corrugation. The minimum of the interaction energy and the corresponding height $z=z_e(x,y)$ for a given lateral position (x,y) is determined from $[\partial E_i(\vec{r})/\partial z]_{x,y}=0$. The lowest value of E_i (or highest adhesion energy) generally occurs when an atom of one commensurate surface faces the hollow (H) site at the other surface. When $|z-z_e|>0$, E_i increases and a normal attractive (repulsive) force acts on the slabs if $z>z_e$ $(z<z_e)$. An external normal force F_N applied to the object sets the separation $\overline{z}(x,y;F_N)$ at a given lateral position (x,y). If one of the commensurate slabs B slides above A under the constant normal force F_N, $z=\overline{z}(x,y;F_N)$ and $E_i(x,y,\overline{z})$ varies with the lateral position. The corrugation of E_i under the constant normal force is the prime cause of friction since it leads to the lateral force

$$\vec{F}_L=-\left\{\left[\frac{\partial E_i}{\partial x}\right]_{z=\overline{z}}\vec{i}+\left[\frac{\partial E_i}{\partial y}\right]_{z=\overline{z}}\vec{j}\right\}. \tag{1}$$

By definition this force is conservative, but part of it becomes nonconservative owing to the stick-slip motion. During the slip, the part of the energy that is stored during sticking is damped by creating a local, nonequilibrium phonon density. The sliding object normally slips less then a lattice parameter, but at certain conditions it can slip more than a unit cell. The van der Waals interaction between the atoms of the two slabs A and B is weak. However, owing to its longer range, the forces on atoms farther away can be approximated by an integral over body forces. This gives a relatively strong but essentially uncorrugated attraction. Consequently, the long-range interaction does not contribute directly to the corrugation of F_L, except that it affects the magnitude of the applied normal force. The above arguments are given for a general case in two-dimensions, but they can apply also to the one-dimensional friction.

III. MODEL CALCULATIONS

Earlier, various features of friction with various lubricant molecules and atoms have been explored by using classical molecular-dynamics method.[19–21] Even simple models such as Tomlinson's[13] and Frenkel and Kontorova's[14] methods have been useful to study dry sliding friction. The model used in the present study aims to explore the effects of various material parameters on the friction. In particular, the friction and stick-slip motion are analyzed in the presence of local elastic deformation in the perpendicular direction. In this respect, our model described in Fig. 1 is different from earlier models.

The sliding object is represented by a single atom, which is sensitive to the atomic structure and the energy corrugation of the substrate. It has coordinates $\vec{\rho}_t(x_t,z_t)$. A sliding object incorporating several atoms could have contributed to energy damping. This would be only a further elaboration of the present model. The agent that pushes the sliding object has coordinates $\vec{\rho}_D(x_D,z_D)$, where $z_D=z_t$. Note that the

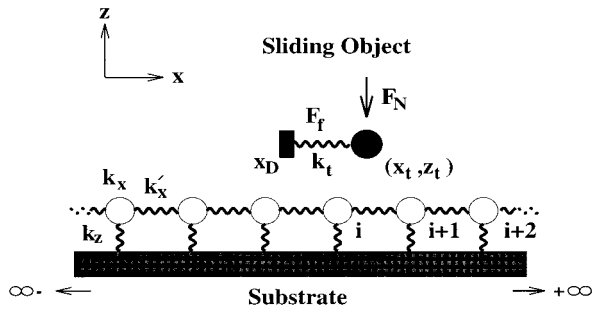

FIG. 1. Atomic model used to study the friction force F_f and the stick-slip motion. F_N is the normal loading force, (x_t,z_t) are the coordinates of the moving agent represented by a single atom, x_D is the position of the moving agent, and k_t, k_x, k_x', and k_z are the spring constants described in the text.

motion of atoms occurs in the lateral (x) and perpendicular (z) directions. The lateral force, acting on the sliding atom is given by $F_L=k_t(x_t-x_D)$ (assuming that $F_L=0$ for $x_D=x_t$), which corresponds to the friction force. The interaction potential between the sliding atom and substrate atoms $V_{ti}(|\vec{\rho}_t-\vec{\rho}_i|)$ are represented by a Lennard-Jones pair potential having parameters $\epsilon=0.84$ eV and $r_0=2.56$ Å. Those parameters are fitted to the physical properties of the Ni metal. The substrate is modeled by an infinite chain of atoms. This way various edge effects due to the finite size of the substrate are avoided. $\vec{\rho}_i(x_i,z_i)$ and $\vec{\rho}_{0i}(x_{i0},z_{i0})$ denote the equilibrium positions of the chain atoms with and without an interaction due to the sliding object, respectively. The cohesion of the substrate is provided by the interchain potential. The total potential of the whole system (sliding object and the substrate) is given by

$$\begin{aligned}V_T=&\sum_i V_{ti}(|\vec{\rho}_t-\vec{\rho}_i|)+\frac{1}{2}k_t(x_t-x_D)^2+\sum_i\frac{1}{2}k_x(x_i-x_{i,0})^2\\&+\sum_i\frac{1}{2}k_x'[(x_{i+1}-x_{i+1,o})-(x_i-x_{i,0})]^2+\sum_i V_{p,i}\\&+F_Nz_t.\end{aligned} \tag{2}$$

Here $V_{p,i}$ is the potential of substrate atoms in the perpendicular direction, which is taken to be harmonic, i.e., $V_{p,i}=k_z(z_i-z_{i0})^2/2$. The total potential V_T as expressed in Eq. (2) is reminiscent of the interaction energy E_i discussed in Sec. II. However, the electronic contribution to V_T is robust. The last term in V_T indicates that an external perpendicular force F_N is acting on the sliding atom. This corresponds to the normal loading force

$$F_N=-\sum_i\left[\frac{\partial V_{ti}}{\partial z_t}\right]_{\overline{z_t}} \tag{3}$$

and sets $z_t=\overline{z_t}$ for a given lateral position x_t. Then the equation of motion of the moving atom under the constant normal force is

$$m\ddot{x}_t+\sum_i\partial V_{ti}/\partial x_t|_{z=\overline{z_t}}+F_N\partial\overline{z_t}/\partial x_t+k_t(x_t-x_D)=0. \tag{4}$$

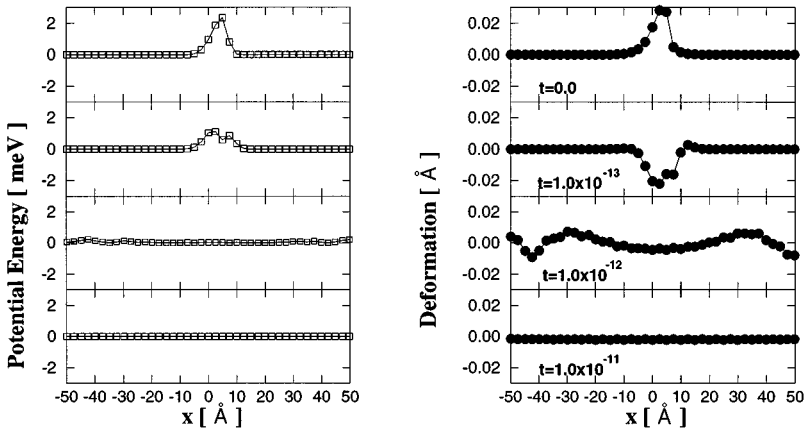

FIG. 2. Propagation of the local potential (strain) energy and deformation created in an infinite 1D substrate. Atoms are allowed to move in the x direction since k_z is taken to be infinite.

Similarly, the equation of motion for the substrate atoms

$$m\ddot{x}_i+\partial V_{ti}/\partial x_i+k_x(x_i-x_{i,0})+2k_x'x_i-k_x'(x_{i+1}+x_{i-1})=0,$$
$$i=0,\pm1,\pm2,\ldots . \quad (5)$$

In the present model, the sliding atom (or object) applies a force to the substrate and induces local deformation. The strain energy stored in this local deformation spreads out in the substrate. This is the path of the energy transfer from the moving object to the substrate leading to the dissipation. Figure 2 illustrates the propagation (dissipation) of the local strain energy and deformation induced by the moving object just before the start of the slip. At this moment the moving object is removed and atoms are allowed to move only in the x direction by taking k_z to be infinite. This can be viewed as the equilibration of a nonequilibrium phonon distribution induced at the close proximity of the tip. The deformation propagates with an average speed of $\sim$3000 m/s. As the speed of the moving object approaches this velocity the dynamical solution becomes important. At this point the following comments are in order. Since the present model has only limited extent in the perpendicular direction, the propagation of the strain energy along the z direction is not considered. The longitudinal and the transversal motion of the substrate atoms are coupled through the two-body potential V_{ti}. However, the transversal motions of atoms become decoupled if they are induced by a local deformation in the absence of the sliding object. As a result, the propogation of the longitudinal mode is not affected in any essential manner by freezing the transversal motion. While part of the mechanical energy transferred from the sliding object to the substrate quickly dissipates through the infinite chain in the longitudinal mode, the remaining part sets vibrations on the atoms left behind the sliding object. In the actual friction, the local deformation creates a local nonequilibrium phonon distribution in the sample as well as in the sliding object. The local strain propogates with the speed of sound and the local nonequilibrium phonon distribution fades away by electron-phonon and mainly phonon-phonon interactions.

In the present study we consider the low sliding speeds in the range of $v_D=dx_D/dt\sim4$ Å/s. This is relevant for the AFM or the FFM. Furthermore, we assume that the normal force F_N does not cause any kind of plastic deformation or wear; hence the energy transferred to the substrate by an induced local deformation spreads with the speed of sound and is dissipated almost suddenly. These conditions justify the quasistatic approximation, in which the friction force F_f at a given time t is equal to the lateral force F_L. This requires the determination of the actual positions of substrate atoms $\{x_i,z_i\}$ for a given x_D and F_N. Since all these coordinates are interrelated through Eq. (2), they can be calculated by using tedious iterative procedures. The calculation of the interaction potential $\Sigma_i V_{ti}$ involves 141 atoms at close proximity to the sliding object. Only 60 atoms out of 141 are allowed to relax under the interaction potentials. The rest of the substrate atoms that are far from the sliding object are kept in their original position since their displacements under the force exerted by the other atoms are insignificant. For x_D at time t we start by determining the equilibrium positions of the atoms for a given (x_t,z_t) by using equilibrium conditions for the forces obtained from the interaction potential. Note that the sliding atom is under the forces F_N, F_L, and the force derived from interaction potential $\Sigma_i V_{ti}(|\vec{\rho}_t-\vec{\rho}_i|)$. In the iteration cycles z_t is varied continuously to find z_t, so that the normal force becomes equal to the desired value F_N. The lateral coordinate x_t of the sliding object is varied to balance F_L. Upon reaching the equilibrium condition at x_D, the friction force F_f, which is equal to F_L, is calculated from the actual values of x_D and x_t. By increasing x_D by $v_D\Delta t$ all steps of iterations are repeated to find F_f for this new value of x_D. This way F_f versus x_D (or F_f versus t) curves are obtained for right sliding or left sliding moving object. This leads to a hysteresis since the average of F_L, $\int_{x_{D1}}^{x_{D2}}F_L dx_D/(x_{D2}-x_{D1})$ is finite and is equal to average friction force F_f.

IV. RESULTS AND DISCUSSION

The stick-slip motion, in particular F_f and the hysteresis curve in dry sliding friction between atomically flat surfaces, is strongly dependent on material parameters (i.e., harmonic and anharmonic terms of the interaction potential) and F_N. In the model described by Fig. 1, the force constant k_t of the sliding object and those of the substrate k_x,k_x',k_z and the interaction potential V_{ti} between the sliding object and the substrate are of crucial importance. The earlier treatments that assumed a rigid substrate surface did not take into account the deformation induced by the moving object. Using the quasistatic approximation, we calculated the hysteresis

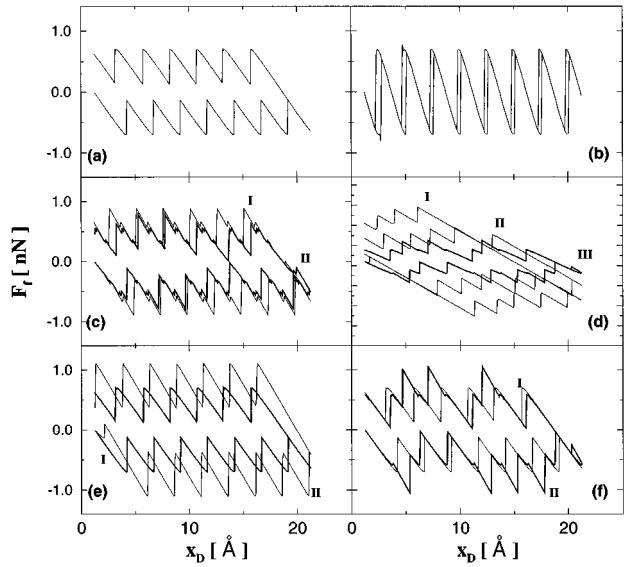

FIG. 3. Hysteresis curves (i.e., variation of F_f in a cycle of x_D) calculated for different material parameters and normal loading force. (a) $F_N=0$ nN; $k_t=0.2$, $k_x=4.3$, $k_x'=5.8$, and $k_z=10$ eV/Å^2. (b) Same as (a) except $k_t=0.8$ eV/Å^2. (c) $F_N=0$; $k_z=10$; $k_t=0.2$ eV/Å^2; I, $k_x=k_x'=1.5$ eV/Å^2; II, $k_x=k_x'=1.7$ eV/Å^2. (d) $F_N=0.2$ nN; $k_x=4.3$; $k_x'=5.8$; $k_t=0.2$ eV/Å^2; I, $k_z=2.5$; II, $k_z=5$; III, $k_z=10$ eV/Å^2. (e) $k_t=0.2$; $k_x=4.3$; $k_x'=5.8$; $k_z=10$ eV/Å^2; I, $F_N=0$ nN; II, $F_N=1$ nN. (f) Same as (e) except II, $F_N=0.2$ nN.

curve [i.e., the $F_f(x_D)$ curve in a cycle of x_D] and examined the effect of material parameters and F_N on the average friction force $\overline{F_f}$. Figure 3 summarizes our results.

According to the definition of friction force in the present model, the elasticity of the sliding object k_t is essential for the stick-slip motion and F_f. In fact, the loss of energy in the course of slipping decreases as k_t increases, and eventually the bistability leading to the slip does not occur when k_t exceeds the value set for a given substrate having the corrugation $F_L(x;F_N)$. In Figs. 3(a) and 3(b) the effect of k_t in the energy damping is seen by comparing the area in the hysteresis curves resulting for two different k_t. For a given k_t, the friction force F_f is strongly dependent on the lateral and perpendicular force constants of the substrate. The energy damping increases with decreasing lateral force constants. For example, by comparing hysteresis curves in Fig. 3(c) one concludes that between two different sets of lateral force constants $k_x, k_x' \simeq 1.5, 1.7$ eV/Å^2 (at fixed loading force $F_N=0$, $k_t=0.2$, $k_z=10$ eV/Å^2) the strongest damping of energy occurs for $k_x, k_x'=1.5$ eV/Å^2. In general, the average energy damping increases with decreasing k_z at a fixed F_N and also with increasing F_N. However, $F_f(k_z)$ at constant F_N and $F_f(F_N)$ at constant k_z are not linear and require a detailed analysis. We present this analysis in Figs. 3–5. The essential aspects of nonlinearity, which were not taken into account before, are the deformation-induced modification of the interaction potential and its anharmonicity. In Fig. 3(d) the hysteresis curves corresponding to $k_z=10$, 5, and 2.5 eV/Å^2 (at $F_N=0.2$ nN, $k_x=4.3$, $k_x'=5.8$, and $k_t=0.2$ eV/Å^2) show that the energy damping (or F_f) increases with decreasing k_z in the range $2.5<k_z<10$. Later in this section we

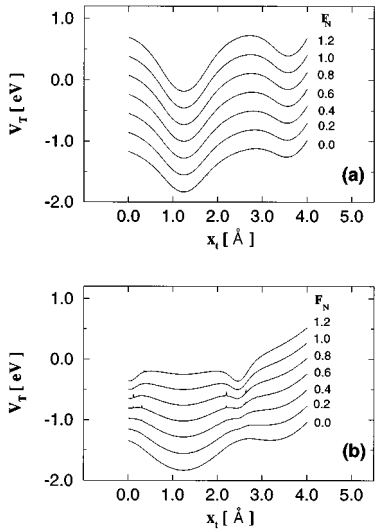

FIG. 4. Total potential V_T versus x_t calculated for various normal forces F_N in nN. (a) Rigid substrate in the perpendicular direction, i.e., $k_z=\infty$ and (b) $k_z=10$ eV/Å^2.

will see that the behavior of $\overline{F_f}(k_z)$ is not straightforward, however. In Figs. 3(e) and 3(f) the hysteresis curves for $F_N=0$, 0.2, and 1 nN (with $k_x=4.3$, $k_x'=5.8$, and $k_t=0.2$ eV/Å^2) show that the energy damping increases with increasing F_N. It is also seen that the stick-slip motion becomes irregular for a certain range of F_N and in the same hysteresis curve two different state stick-slip motions (or some kind of anisotropy) are distinguished. Such an effect dissapears as $k_z\rightarrow\infty$ (i.e., the substrate surface becomes rigid) or the variation of V_T in the perpendicular direction becomes strongly anharmonic. Normally, one expects that the profile of $F_f(x_D)$ is uniform even if $F_N\neq 0$ since the

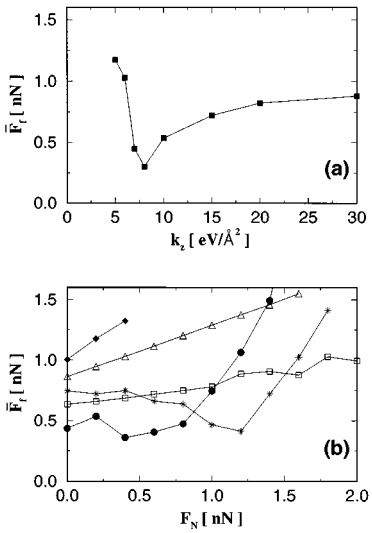

FIG. 5. (a) Variation of the average friction force as a function of force constant in the perpendicular direction k_z. $F_N=0.2$ nN. (b) Average friction force versus normal loading force F_N calculated for various k_z. Filled squares, triangles, stars, filled circles, and empty squares correspond to $k_z=5$, ∞, 15, 10 eV/Å^2, and anharmonic $V_{p,i}$, respectively.

elastic deformation is continuous. However, due to the corrugation inversion, a discontinuous change in the elastic deformation can take place at certain range of F_N. Then the motion makes a transition from one minimum (state 1) to another minimum (state 2). This interesting finding is clarified in Fig. 4(a). As seen, V_T is low at the H site (between two substrate atoms), but increases at the T site (on top of the substrate atom). The corrugation $\Delta V_T = V_T(T) - V_T(H)$ increases with increasing normal force for $k_z \gg 1$. On the other hand, ΔV_T varies with the normal force if the substrate surface is elastic in the perpendicular direction. In Fig. 4(b) the corrugation ΔV_T is positive for $F_N = 0$, but decreases with increasing F_N; eventually the corrugation is inverted at some range of F_N. The inversion of ΔV_T is related with the large elastic deformation of the substrate in the perpendicular direction. Our results predict that the corrugation inversion occurs for substrates that have small k_z for a wide range of perpendicular elastic deformation and are closely related to the second state in the stick-slip motion: For $F_N = 0$, F_f has a well-defined value prior to the slip and the profile of $F_f(x_D)$ is uniform. Our calculations predict that the profile of $F_f(x_D)$ exhibits anisotropy at a certain range of F_N. The range of F_N where anisotropy in the stick-slip motion occurs depends on the value of k_z. Upon the onset of the anisotropy the stick-slip motion makes a transition from the first state ($\Delta V_T > 0$) to a second state ($\Delta V_T < 0$). The onset of the second state is prevented by the anharmonic and strongly repulsive forces opposing the perpendicular deformation. The variation of the average friction force F_f with k_z and F_N are important aspects revealed in the present model. The variation of F_f with k_z with constant F_N is illustrated in Fig. 5(a). F_f has minimum at $k_z \sim 7.5$ eV/Å^2, which can be explained as follows. In the range $k_z < 7.5$ eV/Å^2, F_f increases with decreasing k_z; the softer the material in the perpendicular direction, the higher the energy lost by friction. On the other hand, for $7.5 < k_z < 20$ eV/Å^2 the energy lost due to friction decreases with decreasing k_z. F_f becomes independent of k_z, for very large k_z, where the substrate becomes rigid in the perpendicular direction.

We finally consider the most fundamental aspect i.e., the variation of F_f with F_N. This is usually taken as $F_f = \mu_k F_N$, which is true for the period of sticking. In the range covering several stick-slip periods the dynamic friction constant μ_d may not be constant. The relation between F_f and F_N obtained in our model depending on k_z and anharmonicity of $V_{p,i}$ is illustrated in Fig. 5(b). For a surface that is rigid in the perpendicular direction ($k_z \to \infty$) μ_d is constant, but varies with F_N when k_z is finite. F_f decreases first and then increases with F_N for $k_z \sim 10$ eV/Å^2. This behavior is related to the inversion of corrugation explained above in Fig. 4(b). Depending upon the value of k_z, the minimum of the $F_f(F_N)$ curve occurs at different F_N. For large F_N, the relation becomes linear. At this point we examine the effect of the anharmonic potential of the substrate atoms in the perpendicular direction $V_{p,i}$. The potential including an anharmonic contribution is expressed in terms of a polynomial up to fourth power of the perpendicular displacement $(z_i - z_{i0})$. For small displacements around the equilibrium position $V_{p,i} \sim k_z (z_i - z_{i0})^2/2$. Our calculations in the model described in Fig. 1 show that the anisotropy of the stick-slip motion disappears gradually with an increasing anharmonic contribution in $V_{p,i}$. As a result, the $F_f(F_N)$ curve becomes linear for small loading force F_N. Nevertheless, the nonlinearity appears for large normal loading forces.

V. CONCLUSION

In this paper we investigated dry sliding friction by carrying out calculations of stick-slip motion of a single atom on an infinite atomic chain. The most interesting finding of this study is that owing to the elastic deformation, the interaction energy and the force variations are modified. In particular, for certain circumstances the corrugation of the interaction energy can be inverted. We showed that such a situation may give rise to a second state in the stick-slip motion and anisotropy in the hysteresis curve.

[1] F. P. Bowden and D. Tabor, *Friction and Lubrication* (Methuen, London, 1965).

[2] E. Rabinowicz, *Friction and Wear* (Wiley, New York, 1965).

[3] J. N. Israelachvili, P. M. McGuiggan, and H. M. Homola, Science **240**, 189 (1987).

[4] For current references see, for example, M. Grunze and H. J. Kreuzer, in *Adhesion and Friction*, edited by Editor(s), Springer Series in Surface Sciences Vol. 17 (Springer-Verlag, Berlin, 1989); B. Bhushan, J. N. Israelachvili, and U. Landman, Nature **347**, 607 (1995).

[5] G. Binnig, C. F. Quate, and Ch. Gerber, Phys. Rev. Lett. **56**, 930 (1986); G. Binnig, Ch. Gerber, E. Stoll, T. R. Albrecht, and C. F. Quate, Europhys. Lett. **3**, 1281 (1987).

[6] C. M. Mate, G. M. McClelland, R. Erlandsson, and S. Chiang, Phys. Rev. Lett. **59**, 1942 (1987).

[7] E. Meyer, R. Overney, D. Brodbeck, L. Howald, R. Lüth, J. Frommer, and H. J. Güntherodt, Phys. Rev. Lett. **69**, 1777 (1992).

[8] *Forces in Scanning Probe Methods*, Vol. 286 of *NATO Advanced Study Institute, Series E: Applied Science*, edited by H. J. Güntherodt, D. Anselmetti, and E. Meyer (Kluwer, Dordrecht, 1995).

[9] O. Marti, Surf. Coat. Technol. **62**, 510 (1993).

[10] R. M. Overney, H. Takano, M. Fujihira, W. Paulus, and H. Ringsdorf, Phys. Rev. Lett. **72**, 3546 (1994).

[11] For recent references, see *Physics of Sliding Friction*, Vol. 311 of *NATO Advanced Study Institute, Series E: Applied Science*, edited by B. N. J. Persson and E. Tosatti (Kluwer, Dordrecht, 1996).

[12] H. Matsukawa and H. Fukuyama, Phys. Rev. B **49**, 17 286 (1994).

[13] G. A. Tomlinson, Philos. Mag. **7**, 905 (1929).

[14] J. Frenkel and T. Kontorova, Phys. Z. Sowjet. **13**, 1 (1938); W. Atkinson and N. Cabrera, Phys. Rev. **138**, A763 (1965).

[15] J. B. Sokoloff, Thin Solid Films **206**, 208 (1991); Phys. Rev. B **47**, 6106 (1993).

[16] D. Tomanek, W. Zhong, and H. Thomas, Europhys. Lett. **15**, 887 (1991).

[17] B. N. J. Persson, Phys. Rev. Lett. **71**, 1212 (1993); Phys. Rev. B **50**, 4771 (1994).

[18] T. Gyalog, M. Bammerlin, R. Lüthi, E. Meyer, and H. Thomas, Europhys. Lett. **31**, 269 (1995).

[19] U. Landman, W. D. Luedtke, and A. Nitzan, Surf. Sci. **210**, L177 (1989); U. Landman, W. D. Luedtke, N. A. Burnhan, and R. J. Colton, Science **248**, 454 (1990).

[20] P. A. Thomson and M. O. Robbins, Phys. Rev. A **41**, 6830 (1990); Science **250**, 792 (1990).

[21] J. A. Nieminen, A. P. Sutton, and J. B. Pethica, Acta Metall. Mater. **40**, 2503 (1992); J. A. Nieminen, A. P. Sutton, J. B. Pethica, and K. Kaski, Model. Simul. Mater. Sci. Eng. **1**, 83 (1992).

[22] H. Yoshizawa, P. McGuiggan, and J. N. Israelachvili, Science **259**, 1305 (1993).

[23] J. B. Sokoloff, Phys. Rev. Lett. **71**, 3450 (1993).

[24] A detailed analysis of the short-range interactions based on *ab initio* calculations can be found in S. Ciraci, A. Baratoff, and I. P. Batra, Phys. Rev. B **41**, 2763 (1990); S. Ciraci, in *Basic Concepts and Applications of Scanning Tunneling Microscopy and Related Techniques*, edited by J. Behm, H. Rohrer, and N. Garcia (Kluwer, Dordrecht, 1990), p. 113.